University Library



A gateway to Melbourne's research publications

Minerva Access is the Institutional Repository of The University of Melbourne

Author/s:
Motin, MA;Karmakar, CK;Palaniswami, M

Title:
PPG Derived Heart Rate Estimation during Intensive Physical Exercise

Date:
2019-01-01

Citation:
Motin, M. A., Karmakar, C. K. & Palaniswami, M. (2019). PPG Derived Heart Rate Estimation during Intensive Physical Exercise. IEEE Access, 7, pp.56062-56069. https://doi.org/10.1109/ACCESS.2019.2913148.

Persistent Link:
https://hdl.handle.net/11343/290310

License:
CC BY NC ND

IEEE Access
Multidisciplinary | Rapid Review | Open Access Journal

Received March 7, 2019, accepted April 11, 2019, date of publication May 2, 2019, date of current version May 9, 2019.

*Digital Object Identifier 10.1109/ACCESS.2019.2913148*

# PPG Derived Heart Rate Estimation During Intensive Physical Exercise

**MOHAMMOD ABDUL MOTIN[1], (Student Member, IEEE), CHANDAN KUMAR KARMAKAR[2], (Member, IEEE), AND MARIMUTHU PALANISWAMI[1], (Fellow, IEEE)**

[1]Department of Electrical and Electronic Engineering, University of Melbourne, Melbourne, VIC 3010, Australia
[2]School of Information Technology, Deakin University, Geelong, VIC 3220, Australia

Corresponding author: Chandan Kumar Karmakar (karmakar@deakin.edu.au)

This work was supported by the Australian Research Council (ARC) Discovery Project under Grant DP190101248.

**ABSTRACT** Accurate and reliable estimation of heart rate (HR) from photoplethysmographic (PPG) signals during moderate and vigorous physical activities is a challenging task, since intense motion artifacts can easily disguise the true HR. A novel method for estimating HR from PPG signal, during intensive physical exercise, is presented in this paper. The proposed method employs a recursive Wiener filtering technique for HR estimation from motion artifacts-corrupted PPG signal and simultaneously recorded the triaxial accelerometer signal. The experimental results demonstrated that the average relative error and the average absolute error of the proposed method on a public dataset (IEEE 2015 Signal Processing Cup Database) of 23 PPG recordings were 1.73 and 1.85 beats per minute, respectively. Our proposed approach is faster and more accurate than the existing proposals. Therefore, the proposed algorithm can be a reliable solution for HR estimation from noisy PPG signal.

**INDEX TERMS** Fast Fourier transform, heart rate, motion artifacts, photoplethysmographic signal, recursive Wiener filtering, recursive spectral subtraction.

## I. INTRODUCTION

In recent years, photoplethysmography (PPG) has drawn much attention as it is a simple, low cost and non-invasive technique for measuring heart rate (HR), respiratory rate (RR), blood pressure, oxygen saturation level in blood, blood sugar and so on [1]. In clinical settings, HR is the most commonly measured bio-marker for monitoring cardiac activity. Measuring accurate and reliable HR during physical exercise is also one of the significant features in fitness testing. Although PPG signal is strongly modulated by cardiac frequency, it becomes very difficult to estimate HR during physical exercises due to the motion artifacts (MAs). During physical exercise, the dominant frequency (the frequency at which the maximum power of a signal is captured) of PPG signal presents the effects of MAs instead of cardiac activity, which is shown in the black boxes 'b' and 'd' in the Fig. 1. Therefore, the estimation of dominant frequency from PPG signal does not provide the true HR during exercise (Fig. 1) and consequently, HR estimation from PPG becomes erroneous.

The associate editor coordinating the review of this manuscript and approving it for publication was György Eigner.

The IEEE 2015 Signal Processing Cup challenge public database of PPG during intensive exercise with reference ECG (electrocardiogram) has resulted in a surge of research publications in the area of PPG derived HR estimation. Different methods that have been proposed to estimate HR from PPG during physical exercise by attenuating or removing MAs are blind source separation (e.g. independent component analysis [2], principal component analysis [3], canonical correlation analysis, singular spectrum analysis [4]), adaptive filtering [5]–[7], ensemble empirical mode decomposition [8], spectral subtraction (SS) [9], Kalman filtering [10], [11], ensemble Wiener filtering [12], [13], particle filtering [14], spectral matrix decomposition [15] and iterative adaptive thresholding [16] (Table 1). Previously reported Wiener filtering based HR estimation algorithms [12], [13], [17], did not exploit individual channel of accelerometer (ACM) signal for denoising PPG signal. Instead, all these studies used the resultant ACM signal as noise signature in Wiener filter. To improve the PPG denoising, we have used the individual channel of ACM signal independently through recursive Wiener filter in this work.

In this paper, a novel method, by combining recursive Wiener filtering (RWF) and history tracking based



2169-3536 © 2019 IEEE. Translations and content mining are permitted for academic research only.
Personal use is also permitted, but republication/redistribution requires IEEE permission.
See http://www.ieee.org/publications_standards/publications/rights/index.html for more information.

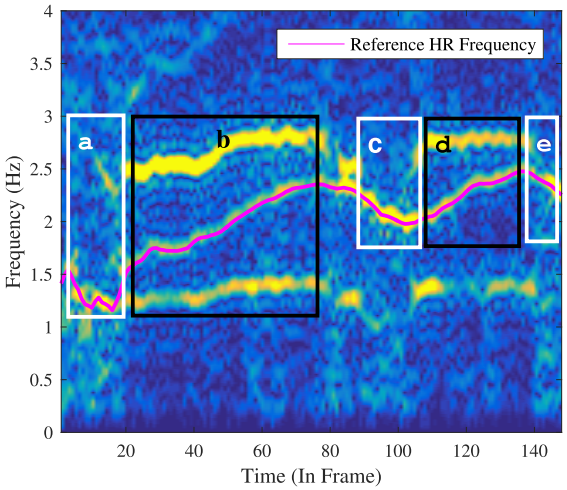



**FIGURE 1.** Time-frequency analysis of raw PPG signal where the RGB color map represents the amplitude information. Ground truth HR frequency curve (showed on magenta) was measured from the reference ECG signal. The dominant frequency of the PPG spectrogram in white boxes 'a', 'c' and 'e' represent the HR activity and black boxes 'b' and 'd' represent the effects of MAs. This figure is generated using short time Fourier transform. We chose 8 second non-overlapping window and the complete recording of eight minutes was segmented into approximately 148 segments. The FFT resolution was chosen 2048 point with the sample rate of 25 Hz.

**TABLE 1.** Methods for extracting HR from PPG during intense exercise.

| Authors | Methods | Signals |
|---|---|---|
| TROIKA [4] | Sparse signal reconstruction | PPG, ACM |
| JOSS [18] | Joint sparse spectrum reconstruction | PPG, ACM |
| MC-SMD [15] | spectral matrix decomposition technique | PPG, ACM |
| IMAT [16] | Iterative adaptive thresholding | PPG, ACM |
| EEMD [19] | Ensemble empirical mode decomposition | PPG, ACM |
| Yang et al. [20] | SS with ensemble empirical mode decomposition | PPG, ACM |
| Fallet *et al.* [21] | Adaptive filtering | PPG, ACM |
| Yalan *et al.* [22] | Nonlinear adaptive filtering | PPG, ACM |
| PARHELIA [14] | Particle filtering | PPG, ACM |
| Temko [12] | Wiener filtering | PPG, ACM |
| SpaMa [9] | Spectral Estimation technique | PPG, ACM |
| Frigo *et al.* [6] | Kalman filtering | PPG |
| Galli *et al.* [10] | Subspace decomposition and Kalman smoothing | PPG, ACM |

post-processing, is presented that shows a better performance than the existing proposals for estimating HR from PPG signal corrupted by intense MAs.

## II. DATABASE AND METRICS

### A. DATABASE

In this study, we used 23 five minute recordings from 20 subjects of ages from 18 to 58 years, which is publicly available in IEEE Signal Processing Cup database [4]. Each recording includes one channel ECG, two channel PPG, and triaxial ACM signals, where all signals are sampled at 125 Hz. The PPG signals were recorded using two wrist-worn pulse

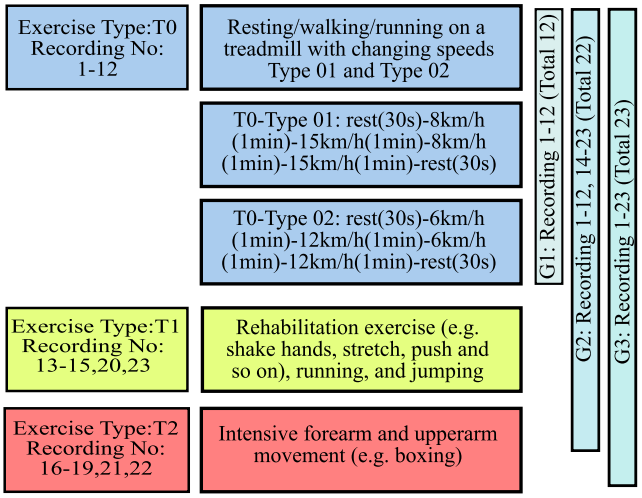



**FIGURE 2.** Recording protocol of IEEE signal processing cup database. Group G1, G2, and G3 have 12, 22, and 23 recordings respectively.

oximeters with green LEDs (wavelength $\sim$ 515 nm). The ACM signals were recorded using a triaxial accelerometer, which was also embedded in the same wristband with pulse oximeter. One channel electrocardiogram (ECG) signal is the ground truth and it is simultaneously recorded with other signals. The ECG signals are reliable enough to be the ground truth because the electrical signals measured from the chest are less affected by MAs. Subjects were engaged with three different types of exercises: 'T0', 'T1', and 'T2' respectively. First twelve (from 1st to 12th) recordings of the database are of 'T0' type exercise where signals are corrupted with less intensive MAs and grouped as 'G1'. The other eleven recordings (from 13th to 23rd) are highly corrupted by MAs since they were acquired during 'T1' and 'T2' type exercises; for them, the HR estimation is more challenging than for the first 12 recordings. For the convenience of comparison with the existing algorithms in the literature, we used the same grouping of recordings: i) G1 (first 12 of 23 recordings); ii) G2 (all 23 recordings except recording $13^{th}$); and iii) G3 (all 23 recordings). The entire outline of the dataset and exercise types is illustrated in Fig. 2.

### B. PERFORMANCE MEASUREMENT

In line with previous studies [4], [9], [10], [18], the average absolute error (*avAE*) and average relative error (*avRE*) metrics are used in this study to measure the performance of HR estimator. *avAE* and *avRE* are defined using equations 1 and 2.

$$avAE = \frac{1}{N}\sum_{n=1}^{N}|HR_{est}(n) - HR_{true}(n)| \quad (1)$$

$$avRE = \frac{1}{N}\sum_{n=1}^{N}\frac{|HR_{est}(n) - HR_{true}(n)|}{HR_{true}(n)} \times 100\% \quad (2)$$

where $N$ is the total number of estimates (number of windows), $HR_{est}(n)$ and $HR_{true}(n)$ denote the estimated and the true HR value in the $n^{th}$ time window in BPM, respectively. In addition to *avAE* and *avRE*, Pearson scatter plot and Bland Altman plot are used as evaluation indexes to demonstrate the similarity and agreement between the reference and the estimated HR.

## III. HEART RATE ESTIMATION AND TRACKING

The algorithm presented in this paper combines three stages of signal processing: 1. Preprocessing of PPG and ACM signals and refining the PPG frequency information using phase vocoder and zero padded DFT. 2. Denoising of PPG signal using recursive Wiener filtering. 3. Smoothing of estimated HR using history tracking. These stages are elaborated in the following subsections.

### A. PREPROCESSING OF PPG AND ACM SIGNALS

The PPG and ACM signals were segmented into 8 seconds window with 75% overlap (6 seconds) and passed through the fourth order Butterworth band-pass filter (0.2-5)Hz. Since the standard sampling rate for extracting HR reliably from PPG must be equal or greater than 25 Hz [23], to reduce the computational cost, we down sampled PPG from 125 to 25 Hz ($1/5^{th}$ of the raw signal) for further processing. Instead of using single channel PPG (either PPG1 or PPG2), we used the averaged value of z-scored (zero mean and unit variance) PPG signals as used in previous studies to reduce unwanted random noise [12], [18].

### B. REFINING PPG FREQUENCY INFORMATION

The frequency resolution of a signal is limited by its window size. For 8 seconds PPG, the frequency resolution is 7.5 ($= 60 \times \frac{1}{8}$) BPM. This resolution is increased by using zero padded DFT. To achieve the HR resolution less than 1 BPM, the minimum frequency shift must be $\nabla_f \leq 1/60$ Hz. In the spectral analysis, the number of FFT bin is set to 2048 which ensures less than 1 BPM frequency resolution.

To get more refined and accurate frequency information, we added phase vocoder technique [24] along with zero padded DFT. Phase vocoder measures the change of phase angle with respect to time to refine the initial estimation of instantaneous frequency [24], [25]. Let us consider, $\theta_1$ and $\theta_2$ are the DFT phases from previous and current frames respectively. We refined the current frequency with the help of previous frequency $f$ using phase vocoder.

$$\arg\min_{n} (f_n - f) \tag{3}$$

$$f_n = \frac{(\theta_2 - \theta_1) + 2\pi n}{2\pi \Delta t}, \quad \forall n \in N;\ f = \frac{d\theta(t)}{2\pi\, dt} \tag{4}$$

where $\Delta t$ is the time difference between two time frames and $f_n$ is calculated for several $n$. In our approach we used $\Delta t = 2$ seconds and $n = 1$ to 10. We chose the value of $f_n$ closest to the previous frequency $f$ and set the new $f = f_n$. Once we get the refined and accurate PPG frequency information using phase vocoder and zero padded DFT, we denoise this PPG using recursive Wiener filtering with the help of triaxial ACM signal.

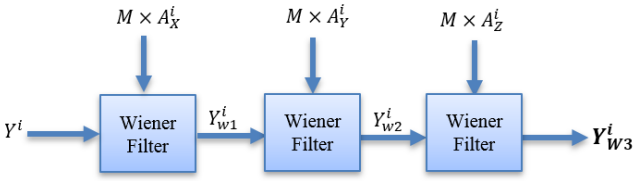



**FIGURE 3.** The overall block diagram of the recursive Wiener filtering. $Y^i$, $Y^i_{W1}$, $Y^i_{W2}$, and $Y^i_{W3}$ are the noisy PPG spectra, filtered output spectra of first, second and final stage respectively for the $i^{th}$ time frame. $A^i_X$, $A^i_Y$, and $A^i_Z$ are the $x$, $y$ and $z$ axis ACM spectra respectively for $i^{th}$ time frame.

### C. RECURSIVE WIENER FILTERING FOR PPG DENOISING

Wiener filter (WF) is an optimal filtering technique to filter out the additive noises from the known stationary noisy signal where filter coefficients are computed by the least square error estimation using the desired signal and filtered estimated signal. In this study, we proposed the RWF approach in the frequency domain to denoise the noisy PPG signal. We used a three stage cascaded WF in the frequency domain with the help of simultaneously recorded ACM signals as the noise signature. The overall block diagram of the proposed RWF approach is shown in Fig. 3. Let us consider $Y^i(f)$ to be the spectra of the $i^{th}$ window of the noisy PPG signal. We denoise $Y^i$ at three different stages with the help of $x, y$ and $z$ axis ACM signal as the noise signature at each stage. The filtered signal of each stage is used as the input for the following stage. Lastly, the filtered output of third stage, $Y^i_{W3}$, is considered as the final denoised signal which is further used to estimate HR. The overall RWF process is defined as:

$$Y^i_{W1} = RW^i_X \times Y^i \tag{5}$$

$$Y^i_{W2} = RW^i_Y \times Y^i_{W1} \tag{6}$$

$$Y^i_{W3} = RW^i_Z \times Y^i_{W2} \tag{7}$$

$Y^i_{W1}$, $Y^i_{W2}$, and $Y^i_{W3}$ are the filtered PPG spectra at $i^{th}$ time frame after first, second and final stage denoising respectively. $RW^i_X$, $RW^i_Y$ and $RW^i_Z$ are the RWF coefficients at $i^{th}$ time frame for first, second and final stage respectively. The RWF coefficients of the proposed approach for each stage are calculated using the following equation:

$$RW^i_P = 1 - \frac{M \times A^i_P}{\frac{1}{min(E,i)} \sum_{j=max(1,i-E+1)}^{i} Y^j} \tag{8}$$

where, $P \in \{X, Y, Z\}$, $M$ is a real valued constant which is used for scaling the noise magnitude, and $A^i_X, A^i_Y$, and $A^i_Z$ are the $x$, $y$ and $z$ axis ACM spectra respectively at $i^{th}$ time frame. In this study, we chose $M = 1/3$ to scale down the noise amplitude. Since we used a three stage RWF, where the filtered output of each stage considered as the input signal for the next stage, one third of the noise amplitude at each stage normalizes the noise magnitude to unit scale.

**Algorithm 1** HR Smoothing Using History Tracking

**Initialization**:
$HR_i = HR\ at\ i-th\ Time\ Frame$;
$N = Total\ of\ Time\ Frames$;
$HR_{LR} = Predicted\ HR\ using\ Linear\ Regression$;
$i_\Theta = 12$;
$\beta = 0.80$;
$HT_1 = 25$;
**while** $i \leq N$ **do**
  **if** $i < i_\Theta$ && $|HR_i - HR_{i-1}| \geq HT_1$ **then**
    $HR_i = \beta HR_i + (1-\beta)HR_{LR}$;
  **else if** $i \geq i_\Theta$ **then**
    $\alpha_i = 0$;
    $n = 1$;
    **while** $n < i - 1$ **do**
      $\Delta = |HR_n - HR_{n+1}|$;
      **if** $\Delta > \alpha_i$ **then**
        $\alpha_i = \Delta$;
    **end**
    $HT_2 = \alpha_i + 3$;
    **if** $|HR_i - HR_{i-1}| \geq HT_2$ **then**
      $HR_i = \beta HR_i + (1-\beta)HR_{LR}$;
**end**

In addition, the average frequency spectrum of previous $E$ spectral envelopes is used as RWF coefficients, which works simply like recursive spectral subtraction (RSS) model when $E = 1$. In this study, we have empirically selected $E = 12$ for calculating RWF output.

### D. HR SMOOTHING USING HISTORY TRACKING

Once the HR is estimated from RWF denoised PPG signal, history tracking is used to smooth the abrupt temporal variation of the estimated HR. The algorithm for history tracking is shown in Algorithm 1. For the first 30 seconds of the recording i.e., for $i-th$ window frame $i < i_\Theta$, estimated HR is considered as the final HR if the difference with respect to previous window frame is less than empirically chosen threshold $HT_1$ $(= 25\ BPM)$. In contrast, if the difference is higher than this threshold, we predict HR from the past five HR estimate using linear regression method.

For HR smoothing after 30 seconds ($i \geq i_\theta$), an adaptive HR threshold ($HT_2$) is estimated from the previously estimated HR trace. Again, if the absolute difference of the estimated HR from the previous HR is $> HT_2$, then we use (9) to predict new HR.

$$\widetilde{HR}_i = \beta \times HR_i + (1-\beta) \times HR_{LR} \tag{9}$$

where $\beta = 0.8$ and $HR_{LR}$ is the predicted HR from the past five HR estimates. Finally, this algorithm provides new HR estimation for every 2 seconds, corresponding to a final reporting rate of 0.5 Hz.

## IV. RESULTS AND DISCUSSION

An example of estimated (using proposed RWF based denoising model) and reference HR from a single subject during 'T0', 'T1' and 'T2' activity is shown in Fig. 4. It is obvious that the reference HR changes abruptly in these subjects and such changes increase with the increased intensity of the activity (see the traces of middle and right panel with respect to the left panel of the Fig. 4). As expected, the proposed model yields exactly similar HR estimation for most of the time frames with the reference HR. The overall performance of the proposed algorithm is demonstrated in the last column of Table 2 and 3. Table 2 and 3 also compare the performance of the proposed algorithm with recently published algorithms. The mean *avAE*, *avRE* values of our algorithm for recording groups G1, G2, and G3 are (1.02, 0.81), (1.78, 1.64) and (1.85, 1.73) BPM respectively. For recording group G1, the proposed algorithm outperforms all previously reported methods except SpaMA enlisted in Table 2 and 3. However, the performance of SpaMA was worse than other studies including our proposed one for groups G2 and G3. This indicates that developing a generalized and performing method to extract HR from PPG during intensive exercise (G2 and G3) is challenging. For the recording groups G2 and G3, our proposed approach outperforms all of the methods listed in Table 2 and 3.

The Pearson correlation (PC) between estimated and actual HR, and the line of best fit (dotted red line) for the recording groups G1, G2, and G3 are shown in Fig. 5 (left panel). The PC values obtained for groups G1, G2 and G3 were 0.997, 0.993, and 0.992 respectively. Additionally, Fig. 5 (right panel) shows the Bland-Altman plot which is used in analyzing the agreement between estimated and ground truth HR. Limit of agreement (LOA) for the recording groups G1, G2, and G3 were [3.46, −3.74], [7.15, −7.01], and [7.30, −7.29] respectively. Pearson correlation coefficients and LOA of Bland-Altman plot showed the robustness of the proposed method in HR estimation.

### A. COMPARISON WITH STATE-OF-THE-ART ALGORITHMS

Most of the studies that used this challenge database reported the results by grouping the recordings in three different groups G1, G2 and G3 (Table 2 & 3). Interestingly, to denoise the PPG signal although most of the studies used accelerometer (ACM) signal, the study [6] neither used ACM signal nor reported HR for intensive noisy recording. This indicates that ACM signal is important in denoising PPG signal during intensive physical activity. In addition, although the best performance reported for group G1 was 0.89 BPM [9] (Table 2), they were 1.90 and 1.97 BPM for groups G2 and G3 respectively [12] (Table 2). This clearly depicts that there is still room for improving the performance of HR estimation during intensive physical activity (groups G2 and G3).

We compared the performance of our algorithm with some of the recently published work PARHELIA [14], Galli *et al.* [10], and Fallet and Vesin [21] along

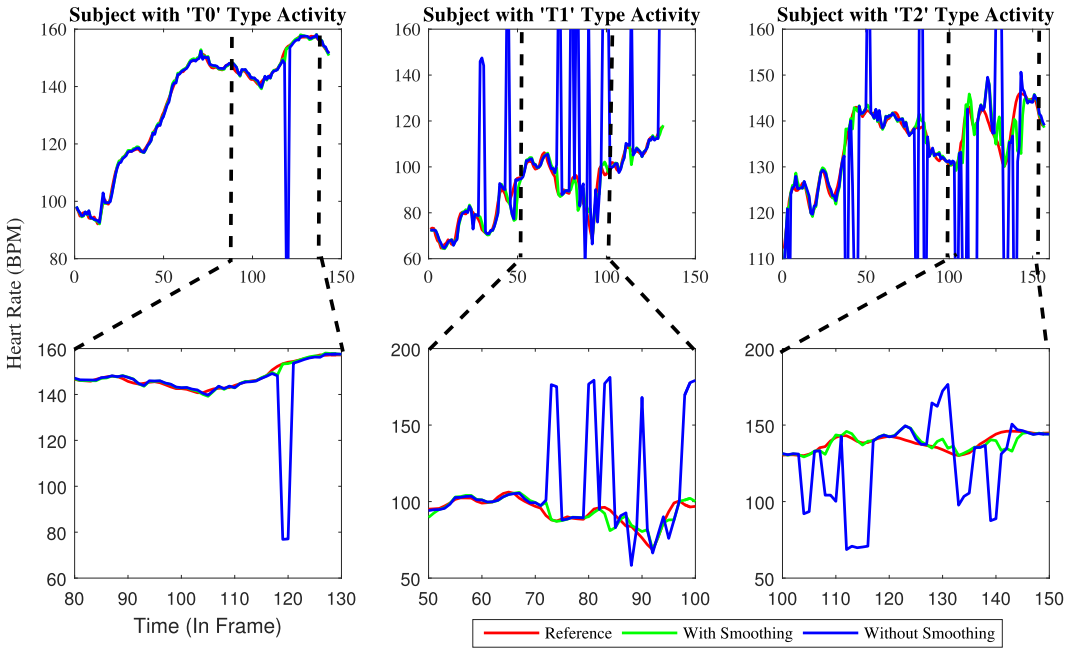



**FIGURE 4.** Continuous heart rate monitoring of one example Subject during 'T0' (left), 'T1' (middle) and 'T2' (right) types of activity using proposed recursive Wiener filter (RWF) based denoising model with and without history tracking based smoothing. The average absolute error of example subject with 'T0', 'T1', and 'T2' type activity was 1.72, 13.75, and 9.96 BPM respectively without smoothing and 0.64, 2.19, and 1.50 BPM respectively with smoothing.

**TABLE 2.** Performance comparison of HR estimation for our proposed method and existing methods in terms of average absolute error *(avAE)* for each recording.

| Recording No | *avAE* | | | | | | | | | |
|---|---|---|---|---|---|---|---|---|---|---|
| | TROIKA [4] | JOSS [18] | IMAT [16] | Temko [12] | MC-SMD [15] | SpaMa [9] | PARHELIA [14] | Fallet *et al.* [21] | Galli *et al.* [10] | **Proposed** |
| 1 | 2.29 | 1.33 | 1.72 | 1.25 | 1.16 | 1.23 | 1.82 | 1.75 | 2.72 | 1.18 |
| 2 | 2.19 | 1.75 | 1.33 | 1.41 | 1.07 | 1.59 | 1.29 | 1.94 | 3.25 | 1.65 |
| 3 | 2.00 | 1.47 | 0.90 | 0.71 | 0.80 | 0.57 | 0.80 | 1.17 | 1.40 | 0.75 |
| 4 | 2.15 | 1.48 | 1.28 | 0.97 | 1.13 | 0.44 | 0.99 | 1.67 | 1.21 | 0.87 |
| 5 | 2.01 | 0.69 | 0.93 | 0.75 | 0.98 | 0.47 | 0.65 | 0.95 | 0.93 | 0.74 |
| 6 | 2.76 | 1.32 | 1.41 | 0.92 | 1.29 | 0.61 | 1.10 | 1.22 | 2.21 | 0.94 |
| 7 | 1.67 | 0.71 | 0.61 | 0.65 | 0.88 | 0.54 | 0.62 | 0.91 | 1.40 | 0.64 |
| 8 | 1.93 | 0.56 | 0.88 | 0.97 | 0.81 | 0.40 | 0.62 | 1.17 | 1.16 | 0.98 |
| 9 | 1.86 | 0.49 | 0.59 | 0.55 | 0.55 | 0.40 | 0.40 | 0.87 | 1.17 | 0.52 |
| 10 | 4.70 | 3.81 | 3.78 | 2.06 | 3.18 | 2.63 | 3.62 | 2.95 | 2.49 | 2.02 |
| 11 | 1.72 | 0.78 | 0.85 | 1.03 | 0.79 | 0.64 | 0.92 | 1.15 | 1.38 | 1.01 |
| 12 | 2.84 | 1.04 | 0.71 | 0.99 | 0.72 | 1.20 | 1.24 | 1.00 | 1.29 | 0.89 |
| 13 | - | - | - | 3.54 | - | 3.41 | - | - | - | 3.38 |
| 14 | 6.63 | 8.07 | - | 9.59 | - | 7.29 | - | 12.12 | 7.91 | 7.66 |
| 15 | 1.94 | 1.61 | - | 2.57 | - | 2.73 | - | 4.02 | 3.65 | 2.06 |
| 16 | 1.35 | 3.10 | - | 2.25 | - | 3.18 | - | 5.64 | 3.90 | 2.12 |
| 17 | 7.82 | 7.01 | - | 3.01 | - | 3.01 | - | 3.31 | 2.44 | 2.77 |
| 18 | 2.46 | 2.99 | - | 2.73 | - | 4.46 | - | 3.39 | 2.14 | 2.84 |
| 19 | 1.73 | 1.67 | - | 1.57 | - | 3.58 | - | 3.45 | 2.60 | 1.50 |
| 20 | 3.33 | 2.80 | - | 2.10 | - | 1.94 | - | 1.56 | 1.86 | 2.19 |
| 21 | 3.41 | 1.88 | - | 3.44 | - | 2.56 | - | 0.95 | 0.85 | 3.58 |
| 22 | 2.69 | 0.92 | - | 1.61 | - | 3.12 | - | 2.52 | 3.06 | 1.56 |
| 23 | 0.51 | 0.49 | - | 0.75 | - | 1.72 | - | 5.86 | 3.38 | 0.77 |
| **Mean G1** | 2.34 | 1.28 | 1.25 | 1.02 | 1.11 | 0.89 | 1.17 | 1.40 | 1.85 | **1.02** |
| **Mean G2** | 2.73 | 2.08 | – | 1.90 | – | 2.01 | – | 2.71 | 2.45 | **1.78** |
| **Mean G3** | – | – | – | 1.97 | – | 2.07 | – | – | – | **1.85** |
| **Std. Dev. G1** | 2.47 | 2.61 | – | 1.25 | 1.99 | – | – | – | 1.88 | **0.44** |
| **Std. Dev. G2** | 0.53 | 0.86 | – | 2.37 | – | – | – | – | 2.83 | **1.56** |
| **Std. Dev. G3** | – | – | – | 2.48 | – | – | – | – | – | **1.57** |

with well-known TROIKA [4] and JOSS [18]. PARHELIA [14], Galli *et al.* [10], Fallet and Vesin [21], TROIKA and JOSS demonstrated mean *avAE* 1.17, 1.85, 1.40, 2.34, and 1.28 BPM respectively for G1 recordings whereas our proposed algorithm showed 1.02 BPM. On the contrary, PARHELIA, IMAT and MC-SMD did not report their

**TABLE 3.** Performance comparison of HR estimation for our proposed method and existing methods in terms of average relative error *(avRE)* for each recording.

| Recording No | *avRE* | | | | | | | | | |
|---|---|---|---|---|---|---|---|---|---|---|
| | TROIKA [4] | JOSS [18] | IMAT [16] | Temko [12] | MC-SMD [15] | SpaMa [9] | PARHELIA [14] | Fallet *et al.* [21] | Galli *et al.* [10] | **Proposed** |
| 1 | 2.18 | 1.19 | 1.50 | 1.15 | 0.91 | 1.14 | - | 1.59 | 2.11 | 1.09 |
| 2 | 2.37 | 1.66 | 1.30 | 1.30 | 0.87 | 1.30 | - | 1.99 | 3.02 | 1.52 |
| 3 | 1.50 | 1.27 | 0.75 | 0.59 | 0.62 | 0.45 | - | 1.02 | 1.11 | 0.63 |
| 4 | 2.00 | 1.41 | 1.20 | 0.88 | 0.84 | 0.31 | - | 1.51 | 1.04 | 0.76 |
| 5 | 1.22 | 0.51 | 0.69 | 0.57 | 0.68 | 0.31 | - | 0.75 | 0.70 | 0.56 |
| 6 | 2.51 | 1.14 | 1.20 | 0.75 | 0.96 | 0.45 | - | 1.05 | 1.82 | 0.76 |
| 7 | 1.27 | 1.09 | 0.50 | 0.50 | 0.65 | 0.40 | - | 0.72 | 1.04 | 0.49 |
| 8 | 1.47 | 0.54 | 0.80 | 0.83 | 0.64 | 0.33 | - | 1.04 | 0.97 | 0.86 |
| 9 | 1.28 | 0.47 | 0.50 | 0.48 | 0.43 | 0.42 | - | 0.76 | 0.95 | 0.45 |
| 10 | 2.49 | 2.43 | 2.40 | 1.29 | 1.95 | 1.59 | - | 1.93 | 2.79 | 1.26 |
| 11 | 1.29 | 0.51 | 0.60 | 0.68 | 0.51 | 0.42 | - | 0.79 | 0.91 | 0.67 |
| 12 | 2.30 | 0.81 | 0.50 | 0.70 | 0.53 | 0.86 | - | 0.79 | 0.92 | 0.64 |
| 13 | - | - | - | 4.08 | - | 4.25 | - | - | - | 3.78 |
| 14 | 8.76 | 10.9 | - | 12.2 | - | 9.80 | - | 16.13 | 10.3 | 9.52 |
| 15 | 2.56 | 2.01 | - | 3.16 | - | 2.21 | - | 5.28 | 4.73 | 2.60 |
| 16 | 1.04 | 2.69 | - | 1.87 | - | 2.11 | - | 2.10 | 2.52 | 1.76 |
| 17 | 4.88 | 4.49 | - | 1.99 | - | 2.52 | - | 3.52 | 1.97 | 1.81 |
| 18 | 2.00 | 2.52 | - | 2.29 | - | 3.23 | - | 2.81 | 1.57 | 2.39 |
| 19 | 1.27 | 1.23 | - | 1.15 | - | 3.98 | - | 2.51 | 2.86 | 1.10 |
| 20 | 3.90 | 3.46 | - | 2.41 | - | 1.66 | - | 4.11 | 1.44 | 2.45 |
| 21 | 2.43 | 1.32 | - | 2.45 | - | 2.02 | - | 3.99 | 0.99 | 2.56 |
| 22 | 2.12 | 0.74 | - | 1.26 | - | 3.28 | - | 1.21 | 2.54 | 1.23 |
| 23 | 0.59 | 0.57 | - | 0.88 | - | 1.97 | - | 1.11 | 2.32 | 0.90 |
| **Mean G1** | 1.82 | 1.01 | 0.99 | 0.81 | 0.80 | 0.65 | – | 1.16 | 1.45 | **0.81** |
| **Mean G2** | 2.33 | 1.91 | – | 1.98 | – | 1.84 | – | 4.28 | 3.13 | **1.64** |
| **Mean G3** | – | – | – | 1.89 | – | 1.95 | – | – | – | **1.73** |

**TABLE 4.** Comparison of the limit of agreement (LOA), Pearson correlation (PC), and computational cost of the proposed method with the existing methods.

| **Methods** | **Group** | **LOA** | **PC** | **Computational Cost** | **Computational Platform** |
|---|---|---|---|---|---|
| TROIKA [4] | G1 | [4.79, - 7.29] | 0.992 | Several sec | Intel Core i7-4790 CPU @ 3.6 GHz, 8GB RAM, Matlab R2013a |
| JOSS [18] | G1 | [5.41, - 5.94] | 0.993 | 600 ms | Intel Core i7-4790 CPU @ 3.6 GHz, 8GB RAM, Matlab R2013a |
| MC-SMD [15] | G1 | [4.13, - 3.68] | 0.996 | – | – |
| IMAT [16] | G1 | [ – , – ] | – | Several sec | Intel Core i7-4930 CPU @ 3.6 GHz |
| EEMD [19] | G1 | [3.98, - 4.10] | 0.996 | 112 ms | Intel Core i7-4790 CPU @ 3.6 GHz, 8GB RAM, Matlab R2013a |
| Fallet *et al.* [21] | G1 | [4.67, - 4.71] | – | – | – |
| PARHELIA [14] | G1 | [5.09, - 4.65] | 0.995 | 27 ms | Intel Xenon X5570 CPU @ 2.93 GHz, Matlab R2015a |
| Galli *et al.* [10] | G1 | [ – , – ] | – | 1600 ms | Intel Core i7, 8GB RAM, Matlab R2015b |
| **Proposed** | G1 | **[3.46, - 3.74]** | **0.997** | **1.13 ms** | Intel Core i7-4790 CPU @ 3.6 GHz, Matlab R2015b |
| Temko [12] | G3 | [8.0, - 7.90] | 0.9908 | 2.90 ms | Intel Core E7200 CPU @ 2.50 GHz, Matlab R2013b |
| **Proposed** | G3 | **[7.30, - 7.29]** | **0.9922** | **1.13 ms** | Intel Core i7-4790 CPU @ 3.6 GHz, 16 GB RAM, Matlab R2015b |

outcomes for G2 and G3 recordings. For G2 recordings, Galli *et al.* [10], Fallet and Vesin [21], TROIKA and JOSS reported 2.45, 2.71, 2.73, and 2.08 BPM mean *avAE* respectively whereas our method exhibited 1.78 BPM. For G3 recordings Temko [12] and SpaMa [9] reported 1.97 and 2.07 BPM mean *avAE* where our algorithm shows 1.85 BPM. The ensemble approach of WF (EWF) [12] showed comparatively better result than other methods listed in table 2 for the recording groups G2 and G3. The proposed RWF based denoising model improves the performance over EWF by 6.31% and 6.10% for the recording groups G2 and G3 respectively. Therefore, the RWF based method is found to be a better solution for HR estimation during intensive physical exercise in the presence of ACM signal as noise signature. In summary, the proposed approach showed better performance than any other well-known and recently published methods listed in Table 2 and 3. Additionally, from Table 2 and 3, it is obvious that none other than Temko [12] and SpaMa [9] so far reported their results (e.g. *avAE* 3.54 and 3.41 BPM respectively and *avRE* 4.08 and 4.25 BPM respectively) for the extremely noisy recording no. 13. Our algorithm demonstrates the best results even for this noisy recording. The *avAE* and *avRE* for recording 13 using our proposed method are 3.38 and 3.78 BPM respectively.

The comparison on LOA of our proposed method with the existing ones is illustrated in Table 4 for recording

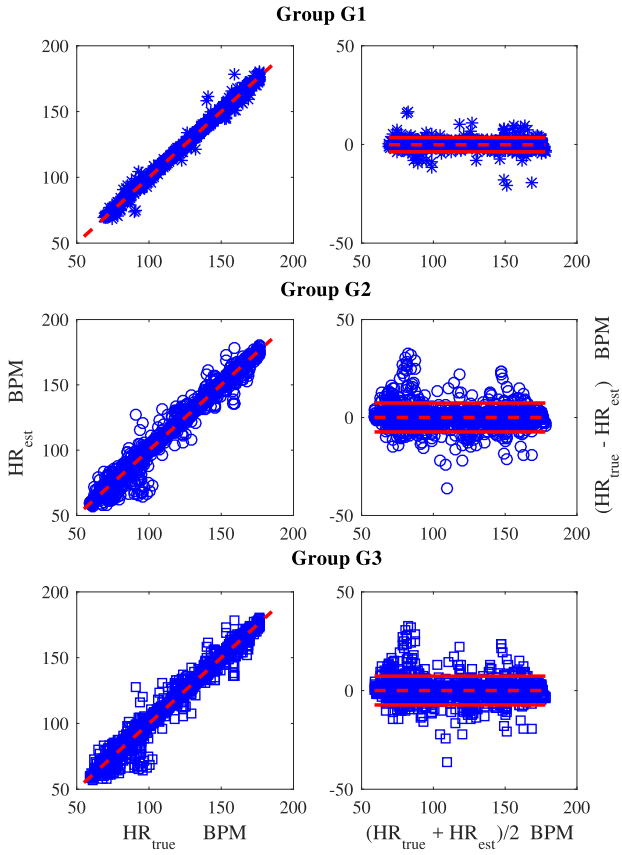



**FIGURE 5.** Pearson scatter plot (left) and Bland Altman plot (right) for recording groups G1, G2, and G3. Pearson correlation coefficients for recording groups G1, G2, and G3 were 0.997, 0.993, and 0.992 respectively. Limit of agreement (LOA) for recording groups G1, G2, and G3 were [3.46, −3.74], [7.15, −7.01], and [7.30 , −7.29] respectively.

group G1. The lower the value of LOA of the Bland-Altman plot, the closer the estimated value to the reference. From Table 4, it is clear that the LOA of our method is smaller than that of other methods mentioned in the table. On the other hand, a higher PC represents higher resemblance between the measured and reference values. The line of best fit will be found when the PC is 1.00. The PC of our proposed method for recording group G1 is 0.997 which is higher than any other methods enlisted in Table 4. Table 4 shows that our proposed method demonstrates both the highest PC and narrowest LOA out of all compared methods. Therefore, the proposed method can estimate HR more accurately and precisely, especially in case of acute physical exercises than all other reported studies.

### B. PROCESSING TIME

The average execution time for all 8 second window was calculated to determine the computational cost of the proposed algorithm which is then used for comparisons against the existing algorithms as shown in the fifth column of Table 4. A limitation of this comparison is of course the differences in the computational platforms; however, the proposed approach is still significantly faster than the state-of-art JOSS.

## V. CONCLUSION

In this paper, we proposed a novel recursive Wiener filtering based denoising algorithm to estimate the heart rate (HR) from photoplethysmography (PPG) signal during intensive physical exercise. The proposed algorithm showed the lowest error rates (1.78 and 1.85) in HR estimation among existing algorithms during intensive exercise (recording groups G2 and G3). In addition, the experimental results for G1 and G2 recordings showed that our algorithm achieved 20.31% and 14.42% better estimation accuracy than the well-known conventional method JOSS. Moreover, the proposed method is also computationally faster than JOSS. Therefore, the proposed algorithm can be an accurate and reliable solution for HR estimation from noisy PPG signal. In the future, we aim to validate the proposed model in estimating HR and breathing rate in real time during daily living activities using wearable computation platforms.

## REFERENCES

[1] J. Allen, "Photoplethysmography and its application in clinical physiological measurement," *Physiol. Meas.*, vol. 28, no. 3, p. R1, 2007.
[2] B. S. Kim and S. K. Yoo, "Motion artifact reduction in photoplethysmography using independent component analysis," *IEEE Trans. Biomed. Eng.*, vol. 53, no. 3, pp. 566–568, Mar. 2006.
[3] M. A. Motin, C. K. Karmakar, and M. Palaniswami, "An EEMD-PCA approach to extract heart rate, respiratory rate and respiratory activity from PPG signal," in *Proc. 38th Annu. Int. Conf. IEEE Eng. Med. Biol. Soc. (EMBC)*, Aug. 2016, pp. 3817–3820.
[4] Z. Zhang, Z. Pi, and B. Liu, "TROIKA: A general framework for heart rate monitoring using wrist-type photoplethysmographic signals during intensive physical exercise," *IEEE Trans. Biomed. Eng.*, vol. 62, no. 2, pp. 522–531, Feb. 2015.
[5] R. Yousefi, M. Nourani, S. Ostadabbas, and I. Panahi, "A motion-tolerant adaptive algorithm for wearable photoplethysmographic biosensors," *IEEE J. Biomed. Health Informat.*, vol. 18, no. 2, pp. 670–681, Mar. 2014.
[6] G. Frigo *et al.*, "Efficient tracking of heart rate under physical exercise from photoplethysmographic signals," in *Proc. IEEE 1st Int. Forum Res. Technol. Soc. Ind. Leveraging Better Tomorrow (RTSI)*, Sep. 2015, pp. 306–311.
[7] M. A. Motin, C. K. Karmakar, and M. Palaniswami, "Robust heart rate estimation during physical exercise using photoplethysmographic signals," in *Proc. 40th Annu. Int. Conf. IEEE Eng. Med. Biol. Soc. (EMBC)*, Jul. 2018, pp. 494–497.
[8] M. A. Motin, C. Karmakar, and M. Palaniswami, "Ensemble empirical mode decomposition with principal component analysis: A novel approach for extracting respiratory rate and heart rate from photoplethysmographic signal," *IEEE J. Biomed. Health Inform.*, vol. 22, no. 3, pp. 766–774, May 2018.
[9] S. M. A. Salehizadeh, D. Dao, J. Bolkhovsky, C. Cho, Y. Mendelson, and K. H. Chon, "A novel time-varying spectral filtering algorithm for reconstruction of motion artifact corrupted heart rate signals during intense physical activities using a wearable photoplethysmogram sensor," *Sensors*, vol. 16, no. 1, p. 10, 2015.
[10] A. Galli, C. Narduzzi, and G. Giorgi, "Measuring heart rate during physical exercise by subspace decomposition and Kalman smoothing," *IEEE Trans. Instrum. Meas.*, vol. 67, no. 5, pp. 1102–1110, May 2018.
[11] A. Galli, G. Frigo, C. Narduzzi, and G. Giorgi, "Robust estimation and tracking of heart rate by PPG signal analysis," in *Proc. IEEE Int. Instrum. Meas. Technol. Conf. (I2MTC)*, May 2017, pp. 1–6.
[12] A. Temko, "Accurate heart rate monitoring during physical exercises using PPG," *IEEE Trans. Biomed. Eng.*, vol. 64, no. 9, pp. 2016–2024, Sep. 2017.

[13] A. Temko, "Estimation of heart rate from photoplethysmography during physical exercise using wiener filtering and the phase vocoder," in *Proc. 37th Annu. Int. Conf. IEEE Eng. Med. Biol. Soc. (EMBC)*, Aug. 2015, pp. 1500–1503.
[14] Y. Fujita, M. Hiromoto, and T. Sato, "PARHELIA: Particle filter-based heart rate estimation from photoplethysmographic signals during physical exercise," *IEEE Trans. Biomed. Eng.*, vol. 65, no. 1, pp. 189–198, Jan. 2018.
[15] J. Xiong, L. Cai, D. Jiang, H. Song, and X. He, "Spectral matrix decomposition-based motion artifacts removal in multi-channel PPG sensor signals," *IEEE Access*, vol. 4, pp. 3076–3086, 2016.
[16] M. B. Mashhadi, E. Asadi, M. Eskandari, S. Kiani, and F. Marvasti, "Heart rate tracking using wrist-type photoplethysmographic (PPG) signals during physical exercise with simultaneous accelerometry," *IEEE Signal Process. Lett.*, vol. 23, no. 2, pp. 227–231, Feb. 2016.
[17] A. Temko, "PPG-based heart rate estimation using wiener filter, phase vocoder and viterbi decoding," in *Proc. IEEE Int. Conf. Acoust., Speech Signal Process. (ICASSP)*, Mar. 2017, pp. 1013–1017.
[18] Z. Zhang, "Photoplethysmography-based heart rate monitoring in physical activities via joint sparse spectrum reconstruction," *IEEE Trans. Biomed. Eng.*, vol. 62, no. 8, pp. 1902–1910, Aug. 2015.
[19] E. Khan, F. Al Hossain, S. Z. Uddin, S. K. Alam, and M. K. Hasan, "A robust heart rate monitoring scheme using photoplethysmographic signals corrupted by intense motion artifacts," *IEEE Trans. Biomed. Eng.*, vol. 63, no. 3, pp. 550–562, Mar. 2016.
[20] Y. Zhang, B. Liu, and Z. Zhang, "Combining ensemble empirical mode decomposition with spectrum subtraction technique for heart rate monitoring using wrist-type photoplethysmography," *Biomed. Signal Process. Control*, vol. 21, pp. 119–125, Aug. 2015.
[21] S. Fallet and J.-M. Vesin, "Robust heart rate estimation using wrist-type photoplethysmographic signals during physical exercise: An approach based on adaptive filtering," *Physiol. Meas.*, vol. 38, no. 2, p. 155, 2017.
[22] Y. Ye, Y. Cheng, W. He, M. Hou, and Z. Zhang, "Combining nonlinear adaptive filtering and signal decomposition for motion artifact removal in wearable photoplethysmography," *IEEE Sensors J.*, vol. 16, no. 19, pp. 7133–7141, Oct. 2016.
[23] A. Choi and H. Shin, "Photoplethysmography sampling frequency: Pilot assessment of how low can we go to analyze pulse rate variability with reliability?" *Physiol. Meas.*, vol. 38, no. 3, p. 586, 2017.
[24] M. S. Puckette and J. C. Brown, "Accuracy of frequency estimates using the phase vocoder," *IEEE Trans. Speech Audio Process.*, vol. 6, no. 2, pp. 166–176, Mar. 1998.
[25] A. Temko, W. Marnane, G. Boylan, and G. Lightbody, "Clinical implementation of a neonatal seizure detection algorithm," *Decis. Support Syst.*, vol. 70, pp. 86–96, Feb. 2015.



**MOHAMMOD ABDUL MOTIN** (S'15) received the B.Sc.Eng. and M.Sc.Eng. degrees in electrical and electronic engineering from the Rajshahi University of Engineering & Technology, Rajshahi, Bangladesh, in 2011 and 2014, respectively. He is currently pursuing the Ph.D. degree with the Department of Electrical and Electronic Engineering, University of Melbourne, Parkville, VIC, Australia. His research interests include biomedical signal processing and modeling, time series analysis, machine learning, embedded systems, and sensor devices for wearable health care monitoring.



**CHANDAN KUMAR KARMAKAR** (M'11) received the B.Sc.Eng. degree in computer science and engineering from the Shah Jalal University of Science and Technology, Sylhet, Bangladesh, in 1999, and the Doctor of Engineering degree from the University of Melbourne, Australia, in 2012. He joined as a Lecturer with the School of Information and Technology, Deakin University, in 2018. He has published one book and more than 130 research articles, including 42 journal articles. His research interests include biomedical devices and signal processing, cardiovascular and neural systems related to sleep-disordered breathing, human gait dysfunctions, cardiovascular diseases, and diabetic autonomic neuropathy.



**MARIMUTHU PALANISWAMI** (F'12) received the M.E. degree from the Indian Institute of Science, Bengaluru, India, in 1977, the M.Eng.Sc. degree from the University of Melbourne, Parkville, VIC, Australia, in 1983, and the Ph.D. degree from the University of Newcastle, Callaghan, Australia, in 1987. He is currently a Professor with the Department of Electrical and Electronic Engineering, University of Melbourne. He has published more than 400 refereed research papers and led one of the largest funded Australian Research Council, Research Network on Intelligent Sensors, Sensor Networks, and Information Processing Program. He has been funded by several ARC and industry grants (over 40 m) to conduct research in vector machine sensors and sensor networks, the IoT, machine learning, neural networks, pattern recognition, signal processing, and control areas. He is representing Australia as a core partner in European Union FP7 projects, such as SENSEI, Smart Santander, the Internet of Things Initiative, and SocIoTal.